INTERNATIONAL JOURNAL FOR NUMERICAL METHODS IN FLUIDS
Int. J. Numer. Meth. Fluids 2005; **47**:803–816
Published online 30 December 2004 in Wiley InterScience (www.interscience.wiley.com). DOI: 10.1002/fld.843

Flow rate defective boundary conditions in haemodynamics simulations

A. Veneziani and C. Vergara*,†

MOX (*Modeling and Scientific Computing*), *Department of Mathematics*, *Politecnico di Milano*, *P.zza L. da Vinci 32*, *20133 Milano*, *Italy*

SUMMARY

In the numerical simulation of blood flow problems it might happen that the only available physical boundary conditions prescribe the flow rate incoming/outgoing the vascular district at hand. In order to have a well-posed Navier–Stokes (NS) problem, these conditions need to be completed. In the bioengineering community, this problem is usually faced by choosing *a priori* a velocity profile on the inflow/outflow sections, that should fit the assigned flow rates. This approach strongly influences the accuracy of the numerical solutions. A less perturbative strategy is based on the so-called 'do-nothing' approach, advocated in Heywood *et al.* (*Int. J. Num. Meth. Fluids* 1996; **22**:325–352). An equivalent approach, however, easier from the numerical discretization viewpoint, has been proposed in Formaggia *et al.* (*SIAM J. Numer. Anal.* 2002; **40**(1):376–401). It is based on an augmented formulation of the problem, in which the conditions on the flow rates are prescribed in a weak sense by means of Lagrangian multipliers. In this paper we extend this analysis to the unsteady augmented NS problem, proving a well-posedness result. Moreover, we present some numerical methods for solving the augmented problem, based on a splitting of the computation of velocity and pressure on one side and the Lagrangian multiplier on the other one. In this way, we show how it is possible to solve the augmented problem resorting to available NS solvers. Copyright © 2004 John Wiley & Sons, Ltd.

KEY WORDS: blood flow simulations; flow rate boundary conditions; Lagrange multipliers

1. INTRODUCTION

In recent years there has been a growing interest in the medical and bioengineering community in the use of numerical simulations of biological systems and devices (see e.g. References [1–3]). In particular, cardiovascular pathologies have a relevant socio-economic impact in

*Correspondence to: C. Vergara, MOX (Modeling and Scientific Computing), Department of Mathematics, Politecnico di Milano P.zza L. da Vinci 32, 20133 Milano, Italy.
†E-mail: christian.vergara@mate.polimi.it

Contract/grant sponsor: EU RTN Project 'Haemodel'; contract/grant number: HPRN-CT-2002-00270

Received 27 April 2004
Revised 13 July 2004
Accepted 26 July 2004

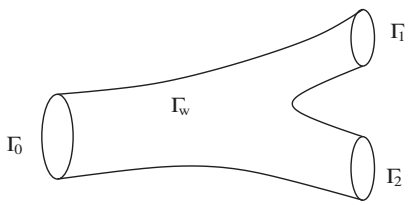

Figure 1. A typical vascular district: the 'physical' boundary (the vascular wall Γ_w) and the 'artificial' boundaries Γ_0, Γ_1 and Γ_2.

Western countries and this has motivated extensive investigations in haemodynamics by means of CFD. For a mathematical introduction to blood flow problems see, e.g. Reference [2].

A relevant problem in the numerical simulation of a vascular district is the prescription of the boundary data. From the mathematical viewpoint, the 3D haemodynamic problem, usually described by the incompressible Navier–Stokes (NS) equations, requires the assignment of three scalar conditions on each boundary point. In practice, these data are often not available on the whole boundary. For the district Ω of Figure 1, for instance, on the boundaries Γ_i $(i = 0, 1, 2)$, i.e. on the interface of the district with the remaining circulatory network, available data often refer to the flow rate, rather than to pointwise velocities. This means that an average datum is prescribed on Γ_i, namely $\int_{\Gamma_i} \rho \mathbf{u} \cdot \mathbf{n} \, d\sigma = Q_i$, $\mathbf{u}$ and ρ being the velocity and the density of the blood, respectively, and with $\mathbf{n}$ the unit normal vector to Γ_i. This condition is clearly not sufficient to generate a well-posed mathematical problem. A similar situation occurs when resorting to the so-called *geometrical multiscale approach* (see Reference [4]), where different mathematical models for the circulation, with a different level of detail, are matched for the simulation of the whole vascular network. In order to complete this defective boundary data set, different techniques have been devised. A quite common strategy consists of selecting *a priori* a velocity profile depending on a parameter to be tuned in order to fulfill flux conditions. In this way, one prescribes standard Dirichlet conditions and the numerical solution strongly depends on the choice of the velocity profile. Recently, different approaches have been proposed with the aim of fulfilling flux conditions in a less perturbative way. In Reference [5], the so-called 'do-nothing' approach is advocated as a possible way for handling both mean pressure drop and flux boundary problems. This approach consists of selecting an appropriate variational formulation, including the given conditions. The natural (homogeneous) boundary conditions, associated with the formulation, automatically complete the defective data set, leading to well-posed problems. This approach has been used in the haemodynamic context for pressure drop problems in References [4, 6, 7]. For the flux problem, a different and more flexible approach has been proposed in Reference [8]. The idea consists of handling flux conditions as a constraint on the solution to be forced in a weak sense via a Lagrange multiplier. In this paper, we move from this approach. In particular, we investigate some theoretical issues concerning the well-posedness of the NS problem 'augmented' by the Lagrange multipliers, thus, completing the analysis in Reference [8] (concerning the steady Stokes problem only). Moreover, we discuss some numerical algorithms for the implementation of this approach while comparing the associated computational costs. In this respect, our viewpoint is to perform a splitting of the augmented problem into the computation of velocity and pressure and the computation of the Lagrange multipliers. With

this approach, the numerical simulations can be performed resorting to available packages (including commercial ones).

The paper is organized as follows. In Section 2 we carry out the well-posedness analysis. We discuss also a different formulation of the problem, based on the curl–curl formulation of the viscous term. In Section 3 we present two possible approaches for the numerical approximation. In Section 4 we provide some numerical results. In particular, the solutions referred to biomedical applications have been obtained with FIDAP (Fluent Inc., U.S.A.), proving the reliability of the augmented approach with commercial ('black-box') solvers.

2. PROBLEM FORMULATION AND ANALYSIS

2.1. The prescribed flux problem

Let us consider a vascular district $\Omega \subset \mathbb{R}^d$ $(d = 2, 3)$ such as that in Figure 1. We assume that blood flow is modelled by the incompressible NS equations for a Newtonian fluid:

$$\begin{aligned} \rho \frac{\partial \boldsymbol{u}}{\partial t} - v \triangle \boldsymbol{u} + \rho(\boldsymbol{u} \cdot \nabla)\boldsymbol{u} + \boldsymbol{\nabla} p = \rho \boldsymbol{f} \\ \nabla \cdot \boldsymbol{u} = 0 \qquad\qquad \boldsymbol{x} \in \Omega,\ t \in (0, T] \\ \boldsymbol{u}|_{t=0} = \boldsymbol{u}_0 \end{aligned} \tag{1}$$

where p is the blood pressure, v the (constant) viscosity, T a prescribed final time (see Reference [2]). In the sequel, for the sake of simplicity, we assume $\rho = 1$. On the physical boundary Γ_w, corresponding to the vascular wall, we assume that the velocity is null, namely $\mathbf{u} = \mathbf{0}$. We are actually assuming that the vascular walls are rigid. This is a simplification, often reasonable in the biomedical context. On the inflow (or more properly 'proximal') boundary Γ_0, and the outflow ('distal') boundaries Γ_j, $j = 1, 2$, we prescribe the flux conditions:

$$\int_{\Gamma_i} \mathbf{u} \cdot \mathbf{n} \, \mathrm{d}\sigma = Q_i, \quad i = 0, 1, 2 \tag{2}$$

In the sequel, we assume that there are $n + 1$ inflow/outflow sections (Γ_i, $i = 0, \ldots, n$) where the flow rate is prescribed. Due to the incompressibility constraint, we need the compatibility condition $\sum_{i=0}^{n} Q_i = 0$ (see Remark below). As pointed out in Section 1, conditions (2) need to be completed in order to have a well-posed problem. The 'do-nothing' approach in Reference [5] suggests that the additional conditions should be automatically selected by choosing an appropriate variational formulation of the problem. Let V denote the Sobolev space $[H^1_{\Gamma_w}(\Omega)]^d$ $(d = 2, 3)$ of the d-dimensional vector functions in $L^2(\Omega)$ together with their first distributional derivatives, vanishing on Γ_w. Let us introduce the space $V^\star = \{\mathbf{v} \in V, \int_{\Gamma_i} \mathbf{v} \cdot \mathbf{n} = 0, i = 0, 1, \ldots, n\}$, and the vector functions $\mathbf{b}_i \in V$, $i = 1, \ldots, n$ (called *flux-carriers*) such that

$$\nabla \cdot \mathbf{b}_i = 0, \quad \int_{\Gamma_0} \mathbf{b}_i \cdot \mathbf{n} \, \mathrm{d}s = -1, \quad \int_{\Gamma_j} \mathbf{b}_i \cdot \mathbf{n} \, \mathrm{d}s = \delta_{ij} \quad \text{for } i, j = 1, \ldots, n$$

where δ_{ij} is the Kroenecker symbol. The weak formulation of the flux problem proposed in Reference [5] reads ($(\cdot, \cdot)$ is the usual L^2 scalar product).

Problem 1
Given $\boldsymbol{f} \in L^2(0,T;L^2(\Omega))$ and $\boldsymbol{u}_0 \in V$, find $\mathbf{u} = \mathbf{w} + \sum_{i=1}^{n} Q_i \mathbf{b}_i$, with $\mathbf{w} \in V^\star$, and $p \in L^2(0,T;L^2(\Omega))$ such that, for all $\mathbf{v} \in V^\star$ and $q \in L^2(\Omega)$

$$\left(\frac{\partial \mathbf{u}}{\partial t} + \mathbf{u}\cdot\nabla\mathbf{u}, \mathbf{v}\right) + \nu(\nabla\mathbf{u}, \nabla\mathbf{v}) - (p, \nabla\cdot\mathbf{v}) = (\boldsymbol{f}, \boldsymbol{v})$$
$$(q, \nabla\cdot\mathbf{u}) = 0 \tag{3}$$

for all $t > 0$, with $\mathbf{u} = \mathbf{u}_0$ for $t = 0$.

It is possible to prove (see Reference [9]) that the implicit 'do-nothing' conditions associated with this formulation are

$$(p\mathbf{n} - \nu\nabla\mathbf{u}\cdot\mathbf{n})_{\Gamma_i} = C_i\mathbf{n} \quad \text{for } i = 0,\ldots,n \tag{4}$$

where C_0 is an arbitrary function of time and the C_i's ($i = 1,\ldots,n$) are *unknown* functions of time (and constant in space).

Remark
As previously pointed out, for the NS problem provided with conditions (2) and null velocity on Γ_w, due to the incompressibility of the fluid, a compatibility condition has to be fulfilled by the data, namely $\sum_{i=0}^{n} Q_i = 0$. This means that only n boundary conditions are actually independent, the last condition (that for the sake of notation we referred to Γ_0) being a consequence of the previous ones. This is the case neither if the walls are compliant nor for a mixed flux/pressure boundary problem. The arbitrary function C_0 in (3) is related to the compatibility condition. Actually, on Γ_0 we are prescribing a condition dependent on the others and we are therefore free to select $C_0 = 0$. Thus, in the sequel, without loss of generality, we will refer to the following boundary conditions:

$$\mathbf{u}|_{\Gamma_w} = \mathbf{0}, \quad (p\mathbf{n} - \nu\nabla\mathbf{u}\cdot\mathbf{n})|_{\Gamma_0} = 0, \quad \int_{\Gamma_i} \mathbf{u}\cdot\mathbf{n}\,\mathrm{d}\sigma = Q_i, \quad i = 1,2,\ldots,n \tag{5}$$

2.2. The augmented reformulation

For the numerical solution of the previous 'do-nothing' approach we need a finite-dimensional subspace of V^*, which might not be easy to construct. We will resort to the formulation proposed in Reference [8], where the conditions on the fluxes are considered as a constraint for the solution, imposed in a weak sense through a set of Lagrange multipliers. In this way, the test functions $\mathbf{v}$ will be taken in a subspace of V, made by standard finite elements. The weak form (3) is thus replaced by

Problem 2
Given $\boldsymbol{f} \in L^2(0,T,L^2(\Omega))$ and $\boldsymbol{u}_0 \in V$, find $\mathbf{u} \in L^2(0,T;V)$, $p \in L^2(0,T;L^2(\Omega))$ and $\lambda_1,\ldots,\lambda_n \in L^2(0,T)$ such that, for all $\mathbf{v} \in V$ and $q \in L^2(\Omega)$,

$$\left(\frac{\partial \mathbf{u}}{\partial t} + \mathbf{u}\cdot\nabla\mathbf{u}, \mathbf{v}\right) + \nu(\nabla\mathbf{u}, \nabla\mathbf{v}) + \sum_{i=1}^{n} \lambda_i \int_{\Gamma_i} \mathbf{v}\cdot\mathbf{n} - (p, \nabla\cdot\mathbf{v}) = (\boldsymbol{f}, \mathbf{v})$$
$$(q, \nabla\cdot\mathbf{u}) = 0$$

$$\int_{\Gamma_i} \mathbf{u} \cdot \mathbf{n} \, \mathrm{d}\sigma = Q_i, \quad i = 1, \ldots, n \tag{6}$$

for all $t > 0$, with $\mathbf{u} = \mathbf{u}_0$ for $t = 0$.

It is possible to prove that the solution $(\mathbf{u}, p, \{\lambda_i\}_{i=1,\ldots,n})$ of Problem 2 coincides with the solution $(\mathbf{u}, p, \{C_i\}_{i=1,\ldots,n})$ of Problem 1 (see Reference [8]).

2.3. *Well-posedness analysis*

The well-posedness analysis of the steady Stokes augmented problem has been carried out in Reference [8] by *superimposition*. This technique relies on the linearity and on the steadiness of the problem (in this case the Lagrangian multipliers are constant). The present analysis refers to the unsteady NS problem, yielding a local-in-time well-posedness result under suitable regularity hypotheses. The analysis is based on some results for Problem 1 (see Reference [5]) as well as on classical results for saddle point problems, that we are going to recall.

Theorem 1 (*see Theorem 7, Heywood et al.* [*5*])
For sufficiently smooth data Q_i with $\sum_i |Q_i|$ and the initial data small enough, Problem 1 is locally well-posed, i.e. there exists a time T^* such that a solution $(\mathbf{u}, p)$ exists for any $t \in [0, T^*]$.

For the next result, we resort to a general abstract problem. Let X and Y be two Hilbert spaces, $b(\cdot, \cdot)$ a continuous bilinear form defined on $X \times Y$, and $a(\cdot, \cdot, \cdot)$ a continuous trilinear form defined on $X \times X \times X$. Let us consider the following problem:

Problem 3
Given $l \in X'$, find $(z, \gamma) \in X \times Y$ such that

$$\begin{aligned} a(z; z, v) + b(v, \gamma) &= \langle l, v \rangle \\ b(z, \mu) &= 0 \end{aligned}$$

for all $v \in X$ and $\mu \in Y$.

Let $W = \{w \in X : b(w, \mu) = 0, \forall \mu \in Y\}$ be the kernel of the bilinear form $b(\cdot, \cdot)$. We can associate Problem 3 with the following 'reduced' problem.

Problem 4
Given $l \in X'$, find $z \in W$ such that $a(z; z, v) = \langle l, v \rangle$ for all $v \in W$.

It is immediate to see that if (z, γ) is a solution of Problem 3, then z is a solution of Problem 4. The converse is true under the following conditions:

Theorem 2 (*see Reference* [*10*])
If the bilinear form $b(\cdot, \cdot)$ fulfils the following inf–sup condition:

$$\exists \beta > 0 : \ \forall \gamma \in Y, \ \exists v \in X : \ b(v, \gamma) \geqslant \beta \|\gamma\|_Y \|v\|_X \tag{7}$$

then, for each solution $z \in X$ of Problem 4, there exists $\gamma \in Y$ such that the couple (z, γ) is a solution of Problem 3.

We can now prove the following result.

Proposition
Under the same regularity assumptions of Theorem 1, Problem 2 is locally well-posed, i.e. there exists a time $T^* > 0$ such that a solution $(\mathbf{u}, p, \{\lambda_i\}_{i=1,\dots,n})$ exists in $[0, T^*]$.

Proof
Assume that $Q_i = 0$ for each i. In this case, observe that Problem 1 and the augmented Problem 2 play the same role of Problems 4 and 3 in Theorem 2, respectively. In the general case of prescribed non-null fluxes, we refer to the velocity field $\tilde{\mathbf{u}} = \mathbf{u} - \sum_i Q_i \mathbf{b}_i$. If $\boldsymbol{\lambda}$ is the vector of the Lagrange multipliers, we can introduce the bilinear form $b(\mathbf{u}, \boldsymbol{\lambda}) = \sum_{i=1}^{n} \lambda_i \int_{\Gamma_i} \mathbf{u} \cdot \mathbf{n}\, d\sigma$. Theorem 1 states that a solution of the reduced problem exists. In order to also prove that the augmented problem is (locally) well-posed, we need to prove that the inf–sup condition (7) is fulfilled for the bilinear form $b(\mathbf{u}, \boldsymbol{\lambda})$. For any n-dimensional vector μ of continuous functions in time and for each $t \in (0, T]$, we set $\|\boldsymbol{\mu}(t)\| = \max_{j=1,\dots,n} \|\mu_j(t)\|$. This definition makes sense, since under the regularity assumptions of Theorem 1, the recovered multipliers will be continuous (in time). Let us denote by $\bar{j}$ $(1 \leqslant \bar{j} \leqslant n)$ the index for which the max is attained (notice that $\bar{j} = \bar{j}(t)$). Set $\mathbf{v} = \mathrm{sign}(\mu_{\bar{j}})(\mathbf{b}_{\bar{j}})$. Recalling that the flux-carriers do not depend on time, we obtain $\forall t \in (0, T]$

$$b(\boldsymbol{\mu}, \mathbf{v}) = \sum_{j=1}^{n} \mu_j \int_{\Gamma_j} \mathrm{sign}(\mu_{\bar{j}}) \mathbf{b}_{\bar{j}} \cdot \mathbf{n}\, d\sigma = \|\boldsymbol{\mu}\| \geqslant \|\boldsymbol{\mu}\| \frac{\|\mathbf{v}\|_V}{\max_j \|\mathbf{b}_j\|_V}$$

For each $t \in (0, T]$, the inf–sup condition is therefore fulfilled with $\beta = 1/\max_j \|\mathbf{b}_j\|_V$ (which is time independent) and the thesis is therefore proved. □

2.4. A different treatment of the viscous term

We can consider a prescribed flux problem with a different treatment of the viscous term (see Reference [11]). By exploiting the vector identity $-\triangle \mathbf{u} = \nabla \times (\nabla \times \mathbf{u}) - \nabla(\nabla \cdot \mathbf{u})$, recalling that $\nabla \cdot \boldsymbol{u} = 0$ and integrating by parts, we obtain

$$-(\triangle \mathbf{u}, \mathbf{v}) = (\nabla \times \mathbf{u}, \nabla \times \mathbf{v}) - \int_{\partial\Omega} ((\nabla \times \mathbf{u}) \times \mathbf{n}) \cdot \mathbf{v}\, d\sigma = (\nabla \times \mathbf{u}, \nabla \times \mathbf{v}) + \int_{\partial\Omega} (\mathbf{v} \times \mathbf{n}) \cdot (\nabla \times \mathbf{u})\, d\sigma$$

So, if we consider the space $\tilde{V} = \{\mathbf{v} \in V, \mathbf{v} \times \mathbf{n}|_{\partial\Omega} = \mathbf{0}\}$, we can formulate the new problem.

Problem 2′
Find $\mathbf{u} \in L^2(0, T; \tilde{V})$, $p \in L^2(0, T; L^2(\Omega))$ and $\lambda_1, \dots, \lambda_n \in L^2(0, T)$ such that, for all $\mathbf{v} \in \tilde{V}$ and $q \in L^2(\Omega)$,

$$\left(\frac{\partial \mathbf{u}}{\partial t} + \mathbf{u} \cdot \nabla \mathbf{u}, \mathbf{v}\right) + \nu(\nabla \times \mathbf{u}, \nabla \times \mathbf{v}) + \sum_{i=1}^{n} \lambda_i \int_{\Gamma_i} \mathbf{v} \cdot \mathbf{n} - (p, \nabla \cdot \mathbf{v}) = (\mathbf{f}, \mathbf{v})$$

$$(q, \nabla \cdot \mathbf{u}) = 0$$

$$\int_{\Gamma_i} \mathbf{u} \cdot \mathbf{n}\, d\sigma = Q_i, \quad i = 1, \dots, n \tag{8}$$

for all $t > 0$, with $\mathbf{u} = \mathbf{u}_0$ for $t = 0$.

In this case it is possible to verify that, besides the flow rates, the conditions induced by the weak form are

$$\boldsymbol{u} \times \boldsymbol{n}|_{\Gamma_i} = 0, \quad p|_{\Gamma_i} = \lambda_i, \quad i = 0, \ldots, n$$

where λ_i are unknown for $i = 1, \ldots, n$ and λ_0 is arbitrary. Observe that in this case the Lagrange multipliers assume a different physical meaning and this could be of some interest, for instance, in the multiscale modelling of the cardiovascular system.

3. NUMERICAL SOLUTION OF THE AUGMENTED PROBLEM

We want now to investigate some numerical methods for the approximation of Problem 3. In the sequel, we refer to a finite element discretization of the NS equations, featuring inf–sup compatible elements. Moreover, we consider a backward difference formulas (BDF) discretization of the time derivatives, with a semi-implicit treatment of the non-linear convective term. Concerning the results provided by our code, we adopt a preconditioned Schur complement solver to compute separately the velocity and the pressure fields (see Reference [12]).

In Reference [8] different methods are proposed to solve the augmented problem, relying on different splitting schemes. As pointed out in Section 1, here we basically refer to splitting methods where the Lagrange multipliers computation can be split from the computation of the velocity-pressure pair. Furthermore, the NS solution is cast in the framework of standard boundary value problems. In this way, the Lagrangian multipliers computation can be coded as an external subroutine for a fluid solver assimilable to a 'black-box'.

Let us denote by V_h and Q_h the subspaces of V and $L^2(\Omega)$ of dimension N_u and N_p and with basis functions will be denoted by ψ_j and ζ_k, respectively. The augmented discrete problem, after an Euler semi-implicit discretization, is given by

$$\begin{bmatrix} K & C^{\mathrm{t}} & \Phi^{\mathrm{t}} \\ C & 0 & 0 \\ \Phi & 0 & 0 \end{bmatrix} \begin{bmatrix} \mathbf{U}^{k+1} \\ \mathbf{P}^{k+1} \\ \boldsymbol{\Lambda}^{k+1} \end{bmatrix} = \begin{bmatrix} \tilde{\mathbf{F}}^{k+1} \\ 0 \\ \mathbf{Q}^{k+1} \end{bmatrix} \tag{9}$$

where $\mathbf{U}^{k+1}$, $\mathbf{P}^{k+1}$ and $\boldsymbol{\Lambda}^{k+1}$ are the vectors of the nodal values of the velocity, the pressure field and of the Lagrange multipliers at time step $k+1$, respectively, $K = (1/\Delta t)M + A + B$ sums up the discretization of the time derivative (mass matrix M) of the viscous term (stiffness matrix A) and of the convective one (matrix B). Finally, $C = [c_{il}] = [(\zeta_l, \nabla \cdot \psi_i)]$, for $l = 1, \ldots, N_p$ and $i = 1, \ldots, N_u$, $\Phi = [\phi_{rj}] = [\int_{\Gamma_r} \psi_j \cdot \boldsymbol{n}\, \mathrm{d}\sigma]$, for $r = 1, \ldots, n$ and $j = 1, \ldots, N_u$, and $\tilde{\mathbf{F}}^{k+1} = \mathbf{F}^{k+1} + (1/\Delta t)M\mathbf{U}^k$, with $\mathbf{F} = [F_i] = (\mathbf{f}, \psi_i)$.

3.1. A GMRes-based scheme

Following Reference [8], we rewrite (9) in a more compact form

$$\begin{bmatrix} S & \tilde{\Phi}^{\mathrm{t}} \\ \tilde{\Phi} & 0 \end{bmatrix} \begin{bmatrix} \boldsymbol{X}^{k+1} \\ \boldsymbol{\Lambda}^{k+1} \end{bmatrix} = \begin{bmatrix} \tilde{\boldsymbol{F}}^{k+1} \\ \boldsymbol{Q}^{k+1} \end{bmatrix} \tag{10}$$

where $S = \begin{bmatrix} K & C^{\mathrm{t}} \\ C & 0 \end{bmatrix}$, $\tilde{\Phi} = \begin{bmatrix} \Phi & 0 \end{bmatrix}$, $\boldsymbol{X}^{k+1} = [\boldsymbol{U}^{k+1} \quad \boldsymbol{P}^{k+1}]^{\mathrm{t}}$ and $\tilde{\boldsymbol{F}}^{k+1} = [\boldsymbol{F}^{k+1} \quad \mathbf{0}]^{\mathrm{t}}$. Since the LBB condition holds, S is non-singular, so we can reduce system (10) by eliminating $\boldsymbol{X}^{k+1}$ as

$$\tilde{\Phi} S^{-1} \tilde{\Phi}^{\mathrm{t}} \boldsymbol{\Lambda}^{k+1} = \tilde{\Phi} S^{-1} \tilde{\boldsymbol{F}}^{k+1} - \boldsymbol{Q}^{k+1} \tag{11}$$

Matrix $R = \tilde{\Phi} S^{-1} \tilde{\Phi}^{\mathrm{t}}$ is the Schur complement associated with (10). It is possible to prove that it is a positive semi-definite matrix (see Reference [8]). Nevertheless, since S is not symmetric in the case of a NS problem, we resort to the GMRes method for the computation of $\boldsymbol{\Lambda}^{k+1}$ (see Reference [13]). To this aim, a system in S has to be preliminarily solved for the computation of $S^{-1}\tilde{\boldsymbol{F}}^{k+1}$. Then, since GMRes converges in at most n iterations (recall that n is the number of sections where flow rate conditions are prescribed, i.e. usually a small number), further n systems in S are solved to compute the residual. Finally, once $\boldsymbol{\Lambda}^{k+1}$ has been computed, a final system in S should be solved for the computation of the velocity and the pressure fields at time t^{k+1}. However, the residual computation in the last GMRes step on the converged solution already entails the solution of the latter system in S, so that the final velocity–pressure computation actually resorts to an algebraic manipulation of vectors. This means that $n+1$ systems in S at each time step are required from this scheme. Moreover, to solve a system for S actually corresponds to the solution of a NS problem with Neumann conditions on the sections where the flow rate is prescribed. This can be pursued by means of a commercial solver.

3.2. *A fixed point algorithm*

An alternative method for the augmented problem is directly inspired by the well-posedness analysis in Reference [8]. For the time being, we refer to the Oseen problem (i.e. to the approximation of the NS problem with an assigned convective field). Let us write the solution as $\mathbf{u} = \tilde{\mathbf{u}} + \sum_{i=1}^{n} \lambda_i(t)\mathbf{w}_i$, $p = \pi + \sum_{i=1}^{n} \lambda_i(t) q_i$, where vectors $\mathbf{w}_i$ and scalars q_i $(i = 1, \ldots, n)$ are the solution of the steady Oseen problems:

$$\begin{gathered} ((\boldsymbol{\beta} \cdot \nabla)\mathbf{w}_i, \mathbf{v}) + (\nabla \mathbf{w}_i, \nabla \mathbf{v}) - (q_i, \nabla \cdot \mathbf{v}) = -\int_{\Gamma_i} \mathbf{v} \cdot \mathbf{n} \, \mathrm{d}\sigma \qquad \forall \mathbf{v} \in V, \forall \psi \in L^2(\Omega) \\ (\psi, \nabla \cdot \mathbf{w}_i) = 0 \end{gathered}$$

The solution of the augmented problem can be regarded as the fixed point of an iterative scheme whose kth iteration reads:

(i) solve $\forall \mathbf{v} \in V, \forall \psi \in L^2(\Omega)$:

$$\begin{aligned} &\left(\frac{\partial \tilde{\mathbf{u}}^{(k+1)}}{\partial t} + (\boldsymbol{\beta} \cdot \nabla)\tilde{\mathbf{u}}^{(k+1)}, \mathbf{v} \right) + \left(\nabla \tilde{\mathbf{u}}^{(k+1)}, \nabla \mathbf{v} \right) - \left(\pi^{(k+1)}, \nabla \cdot \mathbf{v} \right) \\ &\quad = -\sum_{i=1}^{n} \frac{\partial \lambda_i^{(k)}}{\partial t} (\mathbf{w}_i, \mathbf{v}) + (\mathbf{f}, \mathbf{v}) \end{aligned}$$

$$(\psi, \nabla \cdot \tilde{\mathbf{u}}^{(k+1)}) = 0$$

in terms of $\tilde{\mathbf{u}}^{(k+1)}$ and $\pi^{(k+1)}$, with $\tilde{\mathbf{u}} = \mathbf{u}_0$ for $t = 0$;

(ii) solve the linear system (whose non-singularity is proven in Reference [8])

$$\sum_{j=1}^{n} \lambda_j^{(k+1)} \int_{\Gamma_i} \mathbf{w}_i \cdot \mathbf{n}\, \mathrm{d}\sigma = Q_i - \int_{\Gamma_i} \tilde{\mathbf{u}}^{(k+1)} \cdot \mathbf{n}\, \mathrm{d}\sigma$$

This approach resorts to the solution of n steady and 2 unsteady Oseen problems with standard boundary conxditions. In the time discrete NS problem $\boldsymbol{\beta}$ represents the velocity extrapolated by the previous time steps. Moreover, in the case of a steady problem the time derivative of the Lagrange multiplier, which in fact couples the computation of $\tilde{\mathbf{u}}$ and that of λ_i, vanishes and this method converges in one iteration. In the unsteady case a convergence analysis of this scheme does not exist. However, the numerical evidence suggests that it converges.

4. NUMERICAL RESULTS

4.1. Fixed point vs GMRes

In this first set of simulations we aim at validating the augmented approach on analytical test cases. We simulate the flow in an axi-symmetric cylindrical rigid domain with a prescribed flow rate ($Q = 10^{-6}$ m^3/s, $\nu = 3.5 \times 10^{-6}$ m^2/s). We recover the well-known Hagen–Poiseuille profile (see Figure 2, left). Then, we prescribe a sinusoidal-in-time flow ($Q(t) = \cos(2\pi t)10^{-6}$ m^3/s), thus recovering the Womersley solution (Figure 2, middle and right and Table I, top).

In Table I, bottom, we compare the numerical performances of the two numerical schemes in Section 3. As pointed out, in the unsteady case the coupling, due to the time derivative, makes the *fixed point* method more expensive, even if it seems more stable in time, as far as it works with larger time steps. In the sequel, we mainly refer to the GMRes scheme. In Figure 3 (top right, and bottom) we illustrate the results obtained by prescribing a physiological flow rate profile (Figure 3, top left) corresponding to $Q_{\mathrm{tot}} = 4.9$ l/min (i.e. $\approx 0.08 \times 10^{-3}$ m^3/s in I.S. units) with a good qualitative agreement between numerical data and experimental measures (see Reference [14]). A more realistic and complex case has been successfully simulated, referring to a (simplified) geometry of a bypass anastomosis (Figure 4).

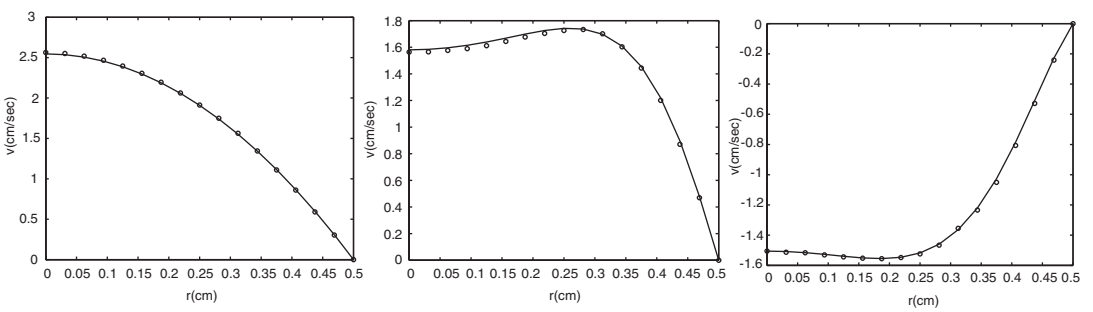

Figure 2. Axial velocity with a constant flux (on the left), with periodic flux at the beginning of the period (middle) and at a half period (right). The markers refer to the numerical solution, continuos line being the analytical one.

Table I. Top: errors (in $L^2(L^2)$ norm) between the numerical and the analytical axial velocity solutions for the pulsatile flow simulation (GMRes Scheme). Bottom: GMRes vs fixed point methods in the unsteady simulations.

	$h = 1/16$	$h = 1/32$
$\Delta t = 0.001$	1.043×10^{-4}	1.211×10^{-4}
$\Delta t = 0.0005$	4.063×10^{-5}	3.679×10^{-5}
	GMRes	Fixed point
CPU time (s)	20.97	486.35
Error ($L^\infty(L^\infty)$)	0.005	0.011
Δt	$\leqslant 0.01$	$\leqslant 0.05$

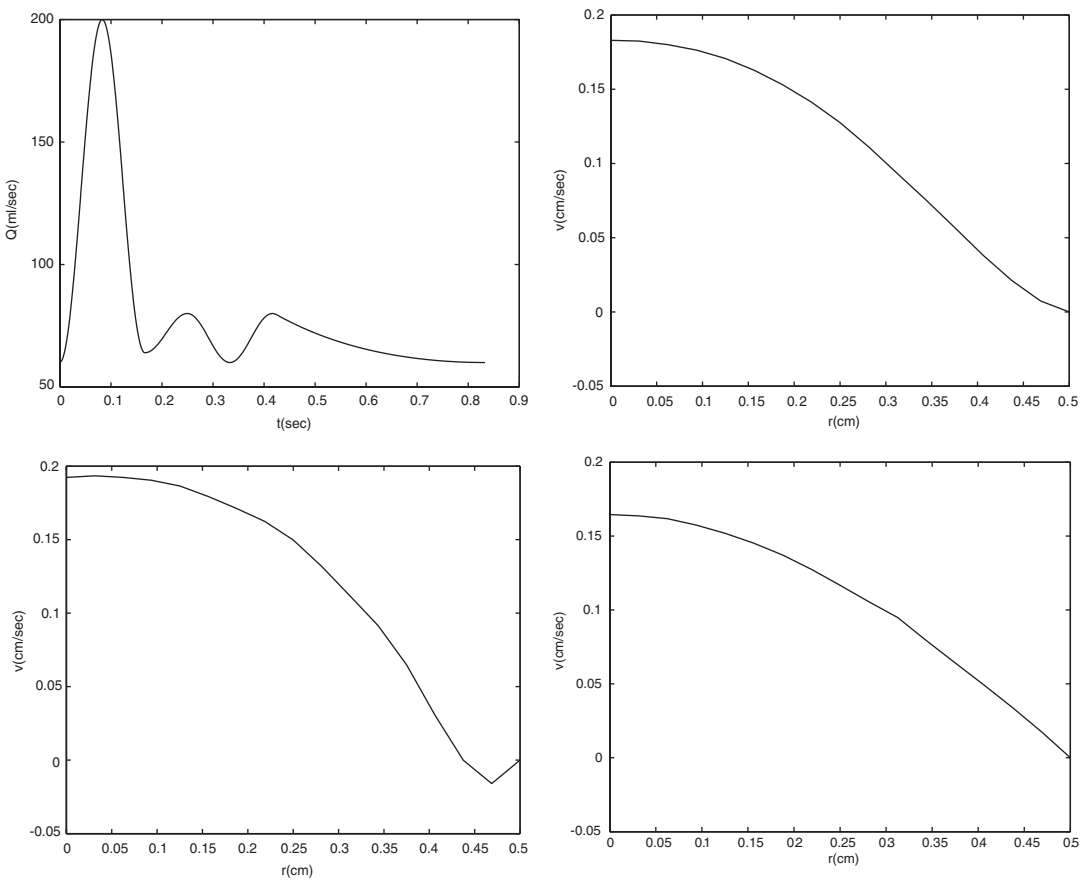

Figure 3. Physiological flow rate profile (top left), corresponding axial velocity at the beginning of the heart beat (top right), at the end of the systole (bottom left) and at the half beat (bottom right).

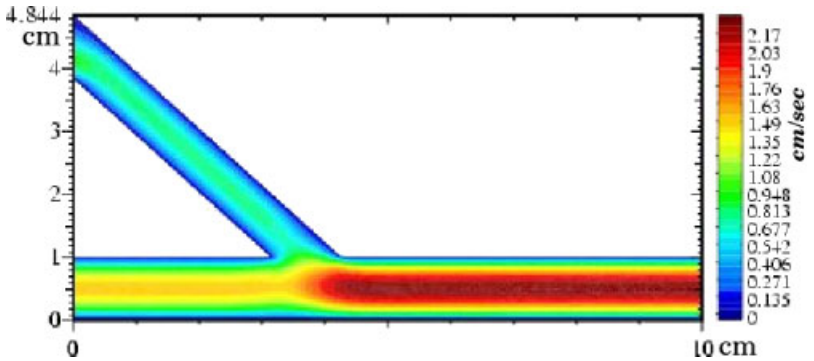

Figure 4. Velocity field in a bypass anastomosis simulation (steady solution).

4.2. Comparison between different formulations of the augmented problem

As pointed out, different variational formulations can be associated with the prescribed flux problem with different 'implicit boundary conditions'. Here, we compare the numerical results obtained with the two formulations provided in Section 2, the one in Equation (6) (grad–grad formulation), and the one in Equation (8) (curl–curl formulation) on a bypass anastomosis. Velocity modulus at different times at the inlet of the bypass (upper branch) are shown in Figure 5 (solid line for 'curl–curl' formulation, markers for the 'grad–grad' formulation). As expected, we have some differences in the solutions, in particular for the pressure (see Table II).

4.3. Multiscale applications

Prescribed flux problems arise also in the (geometrical) multiscale modelling of the circulatory system. In this case (see Reference [15]) a 3D (or 2D) NS solver is coupled with a lumped parameter (LP) model for the whole arterial network. The LP model provides the boundary data to the NS solver and receives a forcing term. LP models are based on an analogy with electric networks and deal with the flow rates and the mean pressure. For instance, the scheme shown in Figure 6 represents a simplified circulatory system, where the pressure generator describes the action of the heart. The boxed part is solved by an NS axi-symmetric solver. In this scheme, the LP model computes the flow rate to be assigned as boundary condition to the NS solver. As a validation, we solve a case in which the heart pumps a periodic pressure both in the multiscale framework and in the complete LP model, where the NS model is replaced by its LP analogue (see Figure 6). We observe that from the viewpoint of systemic simulations the results are in good agreement (see Table in Figure 6), having the possibility in the multiscale framework of detailing the local blood flow features with the 3D model.

4.4. Simulations with a 'black-box' (commercial) solver

We finally illustrate the solution of an augmented problem resorting to the commercial package FIDAP as NS solver. For the sake of simplicity, we refer to the solution of a steady Stokes solver by means of the algorithm of Section 3.2. The application of the GMRes scheme is still under construction. In particular, we refer to the problem of the *total cavopulmonary*

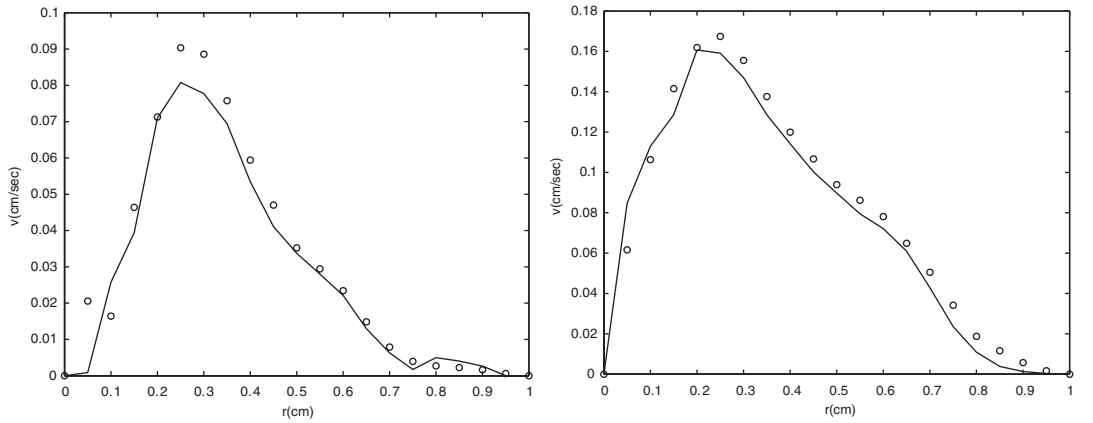

Figure 5. Inlet velocity modulus at the beginning of the time period (left) and at the half period (right) in a bypass simulation with sinusoidal prescribed flux.

Table II. Differences between 'grad–grad' and 'curl–curl' formulations.

$\|\mathbf{u}_{\text{grad}} - \mathbf{u}_{\text{curl}}\|_{L^\infty L^2}$	$\int_{\Gamma_{\text{up}}} \lvert p_{\text{grad}} - p_{\text{curl}} \rvert$
2.16×10^{-4}	5.31×10^{-1}

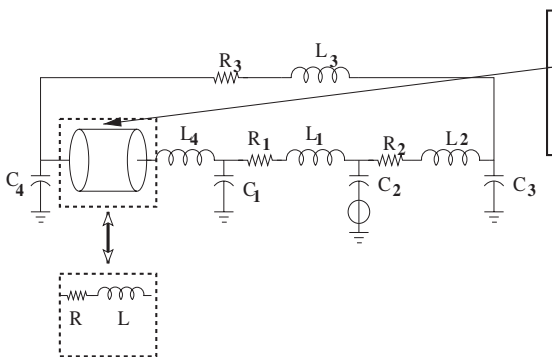

	Multiscale (grad)	Multiscale (curl)	LP
Flux	0.0570	0.0569	0.0593
Pressure	0.1274	0.1234	0.1246

Figure 6. Electrical net modelling of the cardiovascular system. In the dotted boxes the geometry for the NS solver (up) and its analogue in term of LP model (down). In the table, the maximum values of flux and pressures in the three cases.

connection, which is a surgical operation sometimes needed in pediatric pathologies in which only the right ventricle works (see Reference [16]). In this case, the pulmonary artery and the vena cava are connected, leading to a cross-shape domain, as illustrated in Figure 7, left, obtained starting from RNM data. The multiscale approach in this case is mandatory to have realistic boundary data accounting for the whole vascular network. Here, we present some results obtained by prescribing physiological defective flow rate data. Observe from

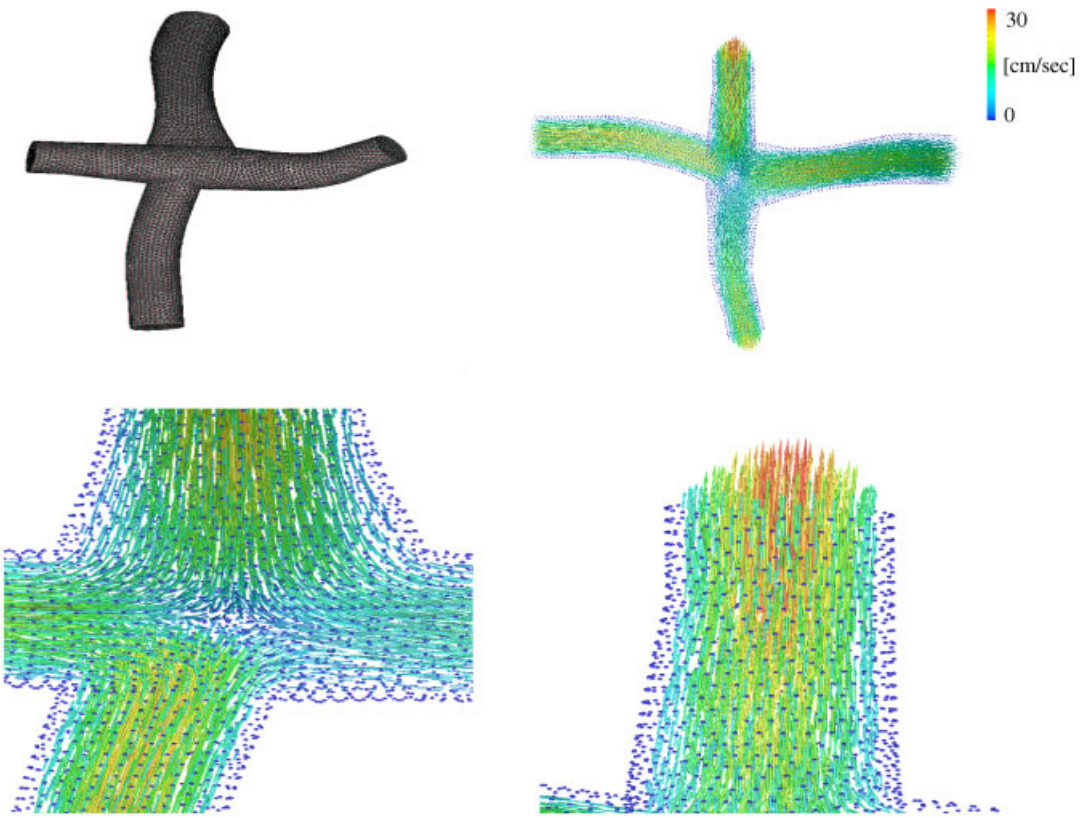

Figure 7. Cavopulmonary connection: the vertical vessel is the Inferior Vena Cava, the horizontal one is the Pulmonary Artery. Computational 3D grid (top, left), velocity field (top, right, bottom left) and on Inferior Vena Cava (bottom, right).

Figure 7, right, how the expected quasi-parabolic profile is obtained as a numerical result of the augmented approach (without prescribing it).

ACKNOWLEDGEMENTS

The authors gratefully acknowledge A. Quarteroni, L. Formaggia, F. Saleri and S. Perotto from MOX and G. Dubini and F. Migliavacca from Laboratory for Biological Structures, Structural Engineering Department, Politecnico di Milano, for many fruitful discussions and suggestions. Part of the simulations has been carried out with a Fortran Code *LIFEII* developed by the authors in cooperation with F. Nobile, S. Deparis, CMCS, EPF Lausanne.

REFERENCES

1. Taylor CA, Draney MT, Ku JP, Parker D, Steele BN, Wang K, Zarins CK. Predictive medicine: Computational techniques in therapeutic decision-making. *Computer Aided Surgery* 1999; **5**(5):231–247.
2. Formaggia L, Quarteroni A. Mathematical modelling and numerical simulation of the cardiovascular system. In *Modelling of Living Systems*, Ayache N, Ciarlet PG, Lions JL (eds). Handbook of Numerical Analysis, Elsevier: Amsterdam, to appear.

3. Quarteroni A, Tuveri M, Veneziani A. Computational vascular fluid dynamics: problems, models and methods. *Computing and Visualisation in Science* 2000; **2**:163–197.
4. Quarteroni A, Ragni S, Veneziani A. Coupling between lumped and distributed models for blood flow problems. *Computing and Visualisation in Science* 2001; **4**:111–124.
5. Heywood J, Rannacher R, Turek S. Artificial boundaries and flux and pressure conditions for the incompressible Navier–Stokes equations. *International Journal for Numerical Methods in Fluids* 1996; **22**:325–352.
6. Veneziani A. Boundary conditions for blood flow problems. In *Proceedings of ENUMATH 97*, Brezzi F *et al*. (eds). World Scientific: River edge, NJ, 1998; 596–605.
7. Quarteroni A, Veneziani A. Analysis of a geometrical multiscale model based on the coupling of ODE's and PDE's for blood flow simulations. *SIAM Multiscale Models Simulation* 2003; **1**(2):173–195.
8. Formaggia L, Gerbeau JF, Nobile F, Quarteroni A. Numerical treatment of defective boundary conditions for the Navier–Stokes equation. *SIAM Journal on Numerical Analysis* 2002; **40**(1):376–401.
9. Veneziani A. Mathematical and numerical modeling of blood flow problems. *Ph.D. Thesis*, University of Milan, 1998.
10. Girault V, Raviart PA. *Finite Element Methods for Navier–Stokes Equations*. Springer: Berlin, 1986.
11. Begue C, Conca C, Murat F, Pironneau O. Les équations de Stokes et de Navier–Stokes avec des conditions aux limites sur la pression. In *Nonlinear Partial Differential Equations and their Applications*, Brezis H, Lions J (eds). College de France Seminar, vol. IX. Pittman Longman: London, 1988; 179–264.
12. Veneziani A. Block factorized preconditioners for high-order accurate in time approximation of the Navier–Stokes equations. *Numerical Methods for Partial Differential Equations* 2003; **19**:487–510.
13. Saad Y. *Iterative Methods for Sparse Linear System*. PWS Publishing Company: Boston, 1996.
14. McDonald D. *Blood Flow in Arteries*. Edward Arnold Ltd: London, 1990.
15. Formaggia L, Nobile F, Quarteroni A, Veneziani A. Multiscale modelling of the circulatory system: A preliminary analysis. *Computing and Visualisation in Science* 1999; **2**:75–83.
16. Migliavacca F, Dubini G, Bove EL, de Leval MR. Computational fluid dynamics simulations in accurate realistic 3-D geometries of the total cavopulmonary anastomosis: The influence of the inferior caval anastomosis. *Journal of Biomechanical Engineering—ASME Transactions* 2003; **125**(6):805–813.
17. Formaggia L, Gerbeau JF, Nobile F, Quarteroni A. On the coupling of 3D and 1D Navier–Stokes equations for flow problems in compliant vessels. *Computational Mathematics in Applied Mechanics and Engineering* 2001; **191**:561–582.

